

Quantification of increased flood risk caused by global climate change for urban river management planning

Etude quantitative de l'augmentation du risque d'inondation sous l'effet des variations climatiques à l'échelle planétaire dans le cadre de la gestion des cours d'eau urbains

Masaru Morita*, Hiroyuki Yamaguchi*

Shibaura Institute of Technology, 3-7-5 Toyosu, Koto-ku, Tokyo 135-8548, Japan (morita@sic.shibaura-it.ac.jp)

RÉSUMÉ

La présente étude décrit une méthode d'analyse quantitative qui montre, dans le cadre de la gestion des cours d'eau urbains, comment les changements climatiques planétaires font augmenter le risque d'inondation. Le concept de « risque d'inondation » (ou « risque inondatoire ») doit être compris ici comme le produit entre le potentiel d'un dommage inondatoire et la probabilité de déclenchement des inondations en question.

L'évaluation du risque d'inondation s'appuie sur un modèle de prévision du dommage inondatoire basé sur un système d'information géographique (SIG). Le modèle que nous avons développé permet de calculer les dommages inondatoires en fonction de chutes de pluies pré-déterminées (et déterminées par différentes années où les chutes de pluie en question dépassent le niveau indiqué). Deux éléments interviennent comme paramètres préalables pour quantifier le risque d'inondation dans le cadre de la présente étude : le dommage subi du fait des chutes de pluie pré-déterminées (exprimé en montants) et la périodicité d'apparition de ces chutes de pluie (ces deux éléments ressortent directement du concept de « risque d'inondation » ci-dessus). Les chutes de pluie pré-déterminées en question ont été établies à partir des résultats de scénarios de simulation des changements de climats planétaires, comme le CGCM2A2 par exemple, et sont exprimées par les formules de la relation « IDF » (Intensité-Durée-Fréquence).

La méthode d'évaluation du risque d'inondation est appliquée ici à la quantification du risque dans le bassin de la rivière *Kanda* à Tōkyō. Cette analyse ne se borne pas à quantifier les augmentations de coûts dus aux risques d'inondation. Elle met en évidence les charges subies par les infrastructures de contrôle des inondations sous l'effet des risques en question.

ABSTRACT

Global climate change is expected to affect future rainfall patterns. These changes should be taken into account when assessing future flooding risks. This study presents a method for quantifying the increase in flood risk caused by global climate change for use in urban flood risk management.

Flood risk in this context is defined as the product of flood damage potential and the probability of its occurrence. The study uses a geographic information system (GIS)-based flood damage prediction model (FDPM) to calculate the flood damage caused by design storms with different return periods. Estimation of the monetary damages these storms produce and their return periods are precursors to flood risk calculations. The design storms are developed from modified intensity-duration-frequency (IDF) relationships generated by simulations of global climate change scenarios (e.g. CGCM2A2).

The risk assessment method is applied to the Kanda River basin in Tokyo, Japan. The assessment provides insights not only into the flood risk cost increase due to global warming, and the impact that increase may have on flood control infrastructure planning.

KEYWORDS

Flood inundation modelling, flood risk assessment, flood risk management, climate change impact.

1 INTRODUCTION

Urban river basins have high flood damage potential because of their concentrated populations and numerous physical and economic assets. National and local governments in Japan have been undertaking structural flood control projects, such as river improvements and the construction of diversion channels and flood control facilities. The available budget for flood prevention is limited and non-structural measures such as flood warnings and evacuations must be undertaken as well. Reasonable and appropriate flood control plans that meet governmental budget requirements as well as provide for the security of the people living in urban river basins must be developed. Thus, the need exists for reasonable engineering methods based on risk assessment that enable decision makers such as municipal engineers and the public officials in charge of flood management to effectively and efficiently evaluate flood control projects (Morita, 2008b; Davis, 2002; Plate, 2002).

There is a widespread consensus that global warming is a real threat to the Earth's future climate (IPCC, 2007). Expected climate change will force decision makers to consider its impact on urban drainage infrastructure and flood control plans. Risk assessment methods should be developed to quantify the increased flood risk under climate change scenarios to provide a rational basis for future plans.

In urban drainage management, design storms are commonly used in the planning of drainage systems. Design storms with characteristic rainfall temporal pattern are obtained from rainfall intensity-duration-frequency (IDF) relationships. Any risk assessment for future planning that uses such design storms should be based on the IDF relationships estimated in anticipation of climate change.

The concepts of risk and risk management have become widely acknowledged among engineers and policy makers both locally (e.g. Guo, 2002) and within the broader context of climate change (DEFRA, 2003). In risk management, the risk of a hazardous event is generally quantified by multiplying the occurrence probability of the event by its impact (National Research Council, 1989). Few flood risk assessment studies have been conducted, however, that strictly follow that concept.

The study presents a risk assessment methodology that deals with the impact of climate change for optimal flood protection planning, relying on standard risk management concepts. The design storms used to develop the assessment come from IDF relationships generated by a simple method of downscaling global climate change scenario simulation results (e.g., CGCM2A2).

2 METHODS

Figure 1 shows the procedure of flood risk assessment applied in this study. It consists of a flood damage prediction model (FDPM) coupled with a risk analysis method. The FDPM simulates the monetary inundation damages produced by given design storms while the risk analysis method quantifies flood risk using three curves: a storm probability curve, a damage potential curve, and a risk density curve.

2.1 Design storms and the storm probability curve

The risk assessment procedure begins with a set of design storms with different return periods specified by a probability distribution. A design storm corresponds to a particular IDF relationship. The design hyetographs for the flood inundation simulations can be generated from IDF relationships using the alternating block method (e.g. Ven Te Chow et al., 1988). The set of hyetographs thus created is input for the flood inundation simulation calculations using Model 1 of the FDPM.

The storm probability curve (Figure 1(a)) shows the relationship of the return period of the design storm and its probability density. Storm level, or the magnitude of design storm, is also expressed in terms of return period.

Global warming is expected to have an impact on precipitation characteristics that will lead to corresponding changes in urban runoff conditions. The temporal patterns of design storms are obtained from the intensity-duration-frequency (IDF) relationships. Thus, IDF relationships estimated bearing climate change in mind are one basic element of a risk assessment that uses the design storms they generate. The method used to generate IDF curves taking global warming into consideration is described in section 3.3.

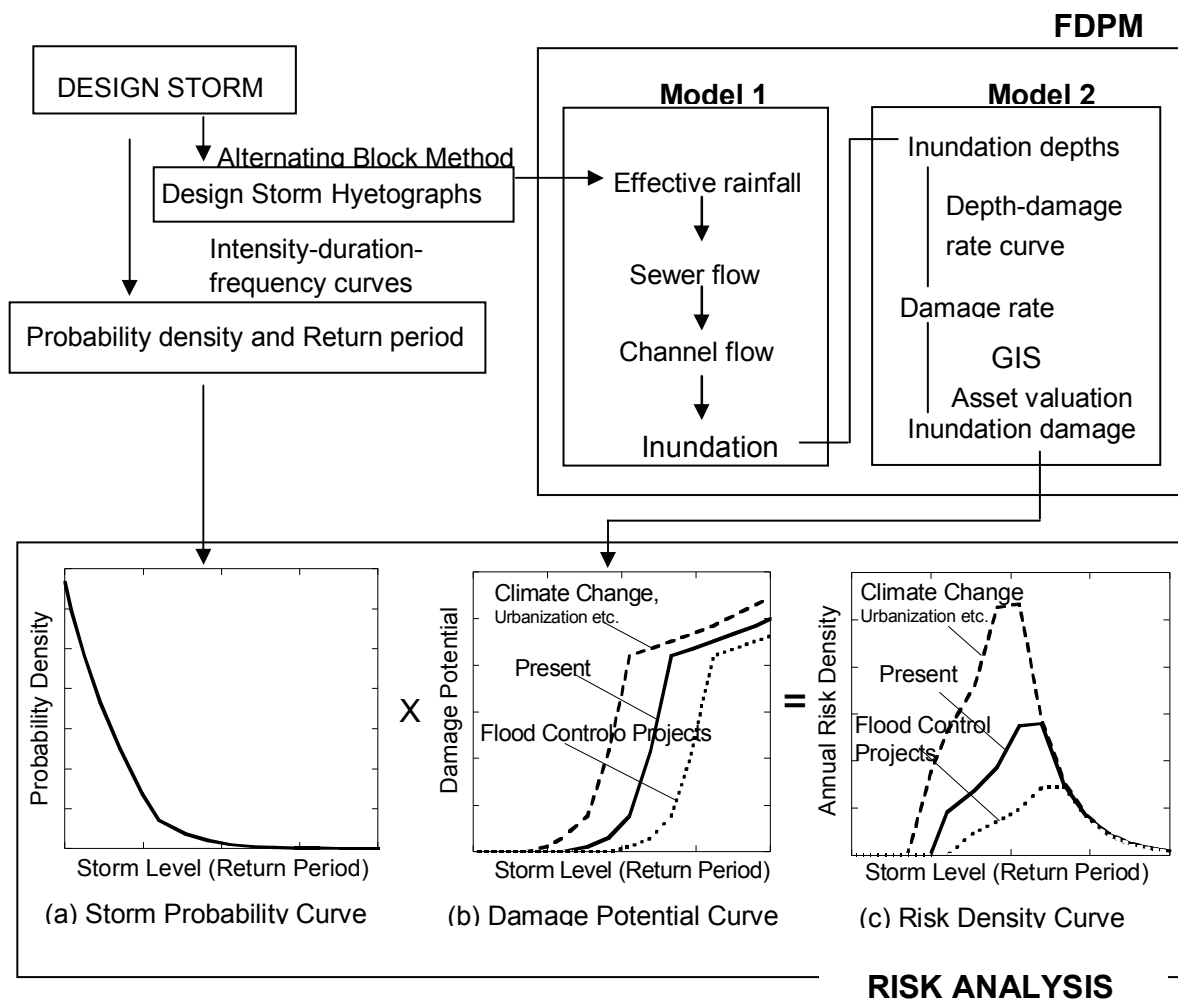


Figure 1. Flood risk assessment procedure with flood damage prediction model (FDPM).

2.2 Flood damage prediction model (FDPM)

The monetary cost of flood damage in a catchment for any given storm or hyetograph can be calculated by a GIS-based flood damage prediction model (FDPM). The FDPM consists of two models: Model 1 and Model 2.

Model 1 calculates the inundation depth on a 50-m square grid for a given storm using the diffusive approximate version of the Saint-Venant equations to simulate one-dimensional sewer and channel flow, and two-dimensional unsteady surface flow (Morita and Yen, 2002). The inundation calculation assumes that the catchment has a natural surface with a roughness coefficient corresponding to an urban area with buildings and roads.

Model 2 is used to estimate the monetary cost of inundation damage as a function of the inundation depth calculated by Model 1 (Morita, 2008a). The monetary damage falls into two categories: direct and indirect damage. Direct damage refers to physical damage to houses, buildings, inventory, public assets and so forth. For example, to calculate the direct damage for each building, we multiply an estimated asset value of the building by a damage rate determined from the inundation depth calculated by Model 1. The interruption to business caused by the direct damage is categorised as indirect damage. Model 2 conforms in general to the manual published by River Bureau of the Construction Ministry (2000) and is described in detail in Morita (2008a).

2.3 Damage potential curve

Flood inundation damages are estimated using Model 1 and Model 2 for any given storm and its probability of occurring. The relationship between the return period of a design storm and the corresponding monetary inundation damage is expressed as a damage potential curve (Figure 1(b)).

The curve, shown by a solid line, represents a damage potential curve for present catchment conditions. Figure 1(b) illustrates the upper and lower damage potential curves. Global warming or urbanization causes increased inundation damage potential as shown by the dashed line. Flood control projects decrease the potential as shown by the dotted line.

2.4 Risk density curve

The concept of “risk” is defined as the product of flood damage and its occurrence probability. Directly applying the definition, using estimates of the monetary damages caused by the design storms and their occurrence probabilities enables us to quantify flood risk as an annual risk density curve.

The annual risk density curve is computed by multiplying the monetary inundation damages by the probability density of the return period. In other words, the increasing damage potential curve (Figure 1(b)) and the decreasing storm probability curve (Figure 1(a)) combine to form the risk density curve which has a peak in the middle (Figure 1(c)). The curve shifts upward for estimates assuming global climate change, as shown by the dashed line, and shifts downward with the application of flood control projects as shown by the dotted line.

2.5 Risk cost and risk cost increase

Risk cost is defined as an expected value of the annual risk density curve and is calculated by integrating the risk density curve with respect to return period. The annual risk cost is monetary expenditure for flood inundation damages averaged over time. As a result, the annual risk cost, or more simply risk cost, increases because heavy storms are expected to become more frequent due to global warming. The risk cost increase caused by climate change is defined as the difference between the present risk cost and the estimated risk cost calculated assuming global warming.

3 APPLICATION OF FLOOD RISK ASSESSMENT

The risk assessment method described above was applied to simulations of the Kanda River basin in Japan's Tokyo metropolitan area. Design storms taking global warming into account were generated based on simulations of global climate change such as CGCM2A2.

3.1 Urban catchment area for flood risk assessment

Figure 2 presents the outline of the Kanda River basin, which has an area of 80.6 km² and is characterised by high population density and numerous physical and economic assets. The basin is extremely urbanized; 65% of its area is impervious. Repeating flooding disasters in low-lying areas since the 1960s have spurred the Tokyo Metropolitan Government to design and install underground flood control reservoirs to reduce the risk of flooding. One example of these projects is the Kanda River underground flood control reservoir under Loop Road 7 (R0 in Figure 2). It was completed in 2006 and has a capacity of 540,000 m³.

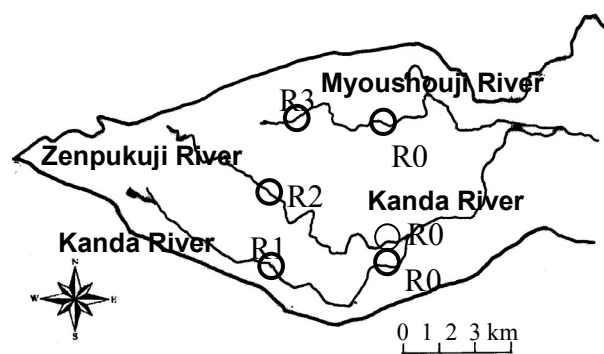


Figure 2. Outline of the Kanda River basin.

The basin has two tributaries: the Zenpukuji River and the Myousyouji River. Three R0s are the inlets of the reservoir under Loop Road 7. R1, R2, and R3 are hypothetical reservoirs.

3.2 Design storms for flood risk assessment

The design hyetographs for the risk assessment were generated based on IDF relationships estimated to represent rainfall patterns altered by global warming.

3.2.1 Storm probability curve for risk assessment

The probability characteristics of the design storms are described as a storm probability curve as shown in Figure 3. The curve shows the relationship between the storm level or return period and the

corresponding probability density. The probability density $f(T)$ for return period T is given by $f(T) = 1/T^2$.

3.2.2 Design hyetograph based on IDF relationship

The Tokyo Metropolitan Government employs the Gumbel distribution, an extreme value distribution which determines the relationship between rain intensity, duration, and the frequency or return period for the flood control planning.

The IDF curves for different return periods representing present conditions are shown in Figure 4(a). The alternating block method was used to create the design hyetographs used by Model 1 in the simulation presented in Figure 4(b). In the inundation simulations, the storm's time step interval, Δt is 10 minutes and the total storm duration T_s is 12 hours.

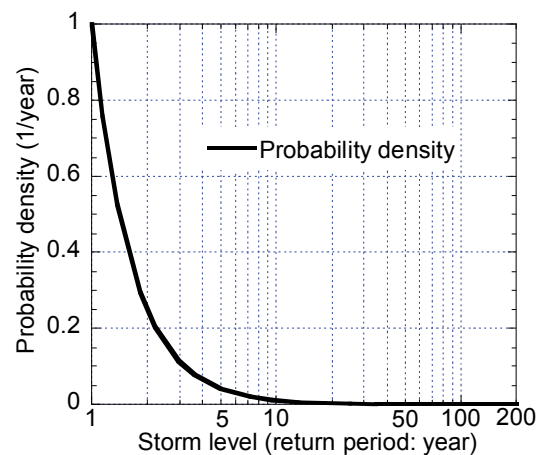


Figure 3. Storm probability curve.

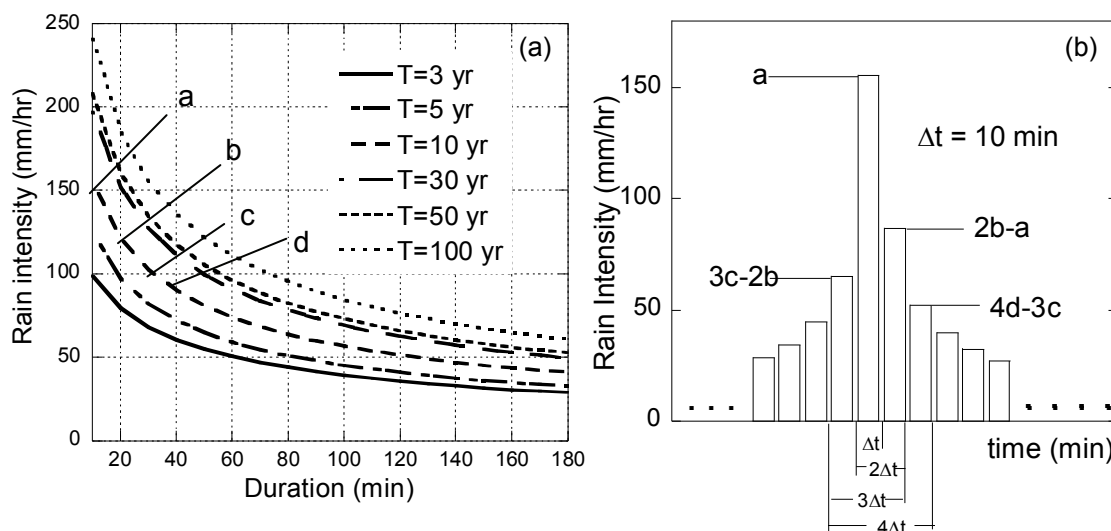


Figure 4. Variation of intensity-duration-frequency (IDF) relationships with return period and example hyetograph created by the alternating block method.

3.2.3 IDF curves for global climate change

Global warming would change the characteristics of storms in the Tokyo area. Some studies (e.g. National Institute for land and infrastructure management (NILIM), 2004; Saita, 2005) have predicted these change based on General Circulation Models (GCMs).

Table 1 Outline of the two studies on global warming

	Research group	verification	prediction	model	predicted change in rain fall
Study A	NILIM	1981 -2000	2031-2050	RCM20	muximum 3-hour rain intensuty etc.
Study B	W.Saita(IIS)	1900 -2000	2000-2100	K-1 Model	annual maximum daily precipitation

The resolution of these GCM outputs, however, is so coarse (280km) that some downscaling should be done to predict GCM climate changes for hydrological impact studies. NILIM (Study A above) studied the variation of rainfall characteristics in the Japan region associated with global warming. The study downscaled the output of CGCM2A2 spatially and temporally to 20km and to a 3-hour duration using a regional climate model (RCM20) developed by the Meteorological Research Institute. They estimated that the maximum 3-hour rain intensity could rise by more than 20%. Saita (2005) of the Institute of Industrial Science (IIS) (Study B above), estimated the annual maximum daily

precipitation for the 20th and 21st centuries in the Tokyo area through probability analysis using the output of the K-1 GCM model. The K-1 model was developed by a joint research group which included the Centre for Climate System Research of Tokyo University (CCSR). The two studies are summarized in Table 1.

In risk assessment, the impact of climate change on the design storms for an urban catchment can be assessed by using the currently used IDF relationships shown in Figure 1 and estimated IDF relationship for the 21st century. The forecast IDF relationships should be estimated incorporating the results of the studies noted above that deal with changes in storm characteristics due to global warming.

Nguyen et al. (2007) gives a detailed description of a spatially-temporal downscaling method and the deviation of the resulting IDF curves. In this study, we adopted a simple method to generate estimated IDF curves for the design storms based on the relationship between the return periods for the 20th and 21st centuries. The IDF relationships for the 20th century are those currently employed by the Tokyo Metropolitan Government. Saita (2005) obtained the relationship shown in the dashed line in Figure 5 by analyzing the probability of precipitation changes forecast for global warming conditions. The IDF relationship for the NILIM (2004) study was also derived from the comparison between the 3-hour extreme rain intensity for the 20th century and that for the 21st century. This relationship is shown by the solid line in Figure 5. The modified IDF curves for the 21st century were obtained from these relationships. Figure 6 shows examples of the estimated IDF curves for a 30-year return period.

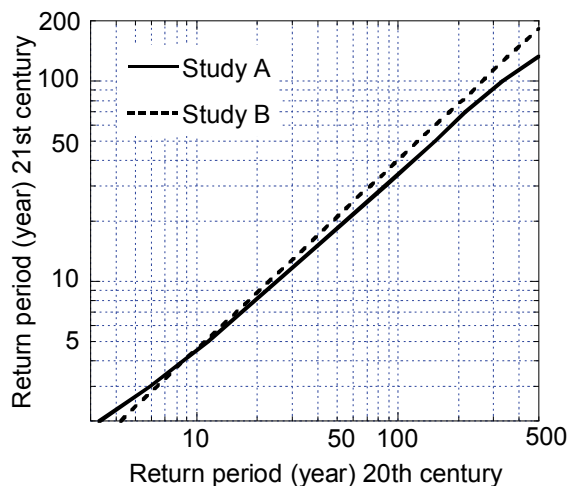


Figure 5. Return periods for 20th and 21st centuries.

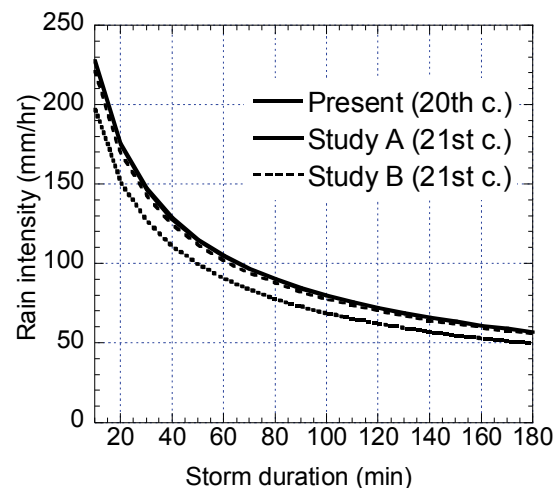


Figure 6. IDF curves for 20th and 21st centuries. (30-year return period storm).

3.3 Flood Inundation damage simulation by Model 1 and Model 2

In the Model 1 simulation, the sewer and the channel flows were calculated one-dimensionally at 50-m intervals. The time increment Δt was set to be 1.0 s for calculation stability. In the two-dimensional inundation depth simulations, a 50-m square grid was adopted mainly because the digital geographical data available from Geographical Survey Institute of Japan are commonly represented at a scale of 50 m. The input design hyetographs were constructed using the alternating block method on the basis of the IDF curves for 2-, 3-, 5-, 15-, 30-, 50-, 70-, 100-, 150-, and 200-year return period storms.

The inundation depths were computed on 50-m square grids using the two-dimensional diffusive wave equation derived from the approximate version of the Saint-Venant equations. The water pathways in the area were not taken into account, and the inundation water was assumed to flow according to the 50-m digital elevation model (DEM).

Figures 7 shows an example of the simulated inundation results for 30-year return period design storms for the estimated 21st century IDF curves (Study A). Increased inundation occurs along the main channel of the Kanda River in Figure 7.

The calculated inundation depths are plotted via GIS and are superimposed on cadastral data for

inundation damage estimated using Model 2 in Figure 8. The GIS data of the Tokyo Metropolitan Government include building asset data as well data on movable assets such as residents and corporations. The asset data for each 50m by 50m square were used to estimate inundation damage, with the damage rate determined from the inundation depth calculated by Model 1.

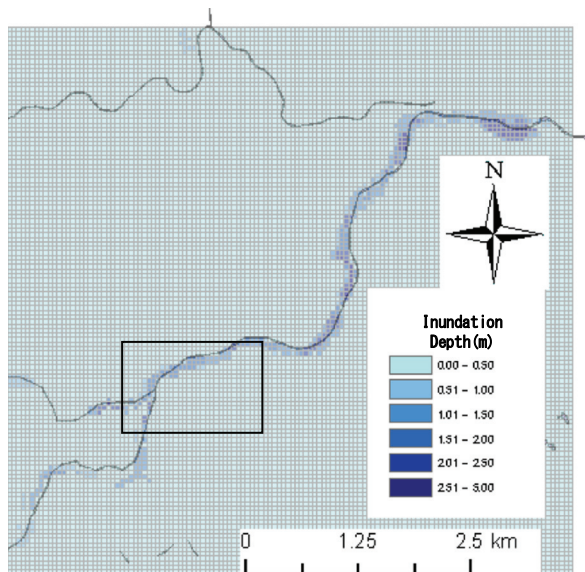


Figure 7. Inundation depth calculated using Model 1. (30-year return period storm for the 21st century IDF curves (Study A)).

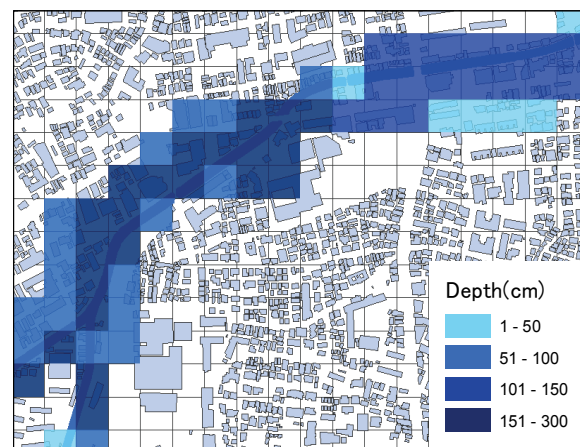


Figure 8. Calculated inundation depth with GIS data superposed for the onset area shown in Figure 7.

The assest data for each 50m by 50m squre square were used to estimate inundation damage with the damage rate determined from the inundation depth calculate d by Model 1.

4 RESULTS AND DISCUSSION

The inundation depths and extent of monetary damage for all grids were calculated using the design storm hyetographs generated from IDF relationships for the 20th century and the 21st century under global warming conditions. The damage potential curves and the annual risk density curves were obtained from the Model 1 and Model 2 simulations.

4.1 Damage potential curve

The total monetary damages associated with the present (20th century) and the modified (21st century) IDF curves are shown in Figure 9. The damages are relatively low when storm levels are low, increasing markedly when specific storm level thresholds—30 years for the 20th century and 15 years for the 21st century—are exceeded. Those specific storm levels inundate the first floor levels of buildings. Figure 9 also indicates that the basin would experience no damage due to inundation by a storm level with a return period of < 5 years for the 20th century and < 3 years for the 21st century. The threat of flooding becomes greater under global warming.

The damage potential curves indicate that the damage for the 21st century is significantly larger than that of the 20th century. The effect of damage increase due to global warming can also be more clearly understood from the three damage potential curves. The two damage potential curves for the 21st century have almost the same trend in terms of damage potential increase with return period, although the damage potential of Study A is a little larger than that of Study B for the storms with greater than 5-year return periods. This is explained by the fact that the estimated return period of Study A over 5-year (y-axis) is a little smaller than that of Study B for the same return period of the 20th century (x-axis) in Figure 5.

4.2 Annual risk density curve

The annual risk density curve was calculated by multiplying the damage potentials due to inundation by the probability densities of storms of different return periods. As shown in Figure 10, annual risk density curves peak at approximately 15 years for the 20th century and 5 years for the 21st century. These arise from the interaction of the decreasing storm probability curve and the increasing damage potential curves. The peak of the annual risk density curve can be considered to be a design storm with the highest flood risk.

Global warming causes a marked increase not only in flood damage potential but also in flood inundation risk. The risk density of Study A is smaller than that of Study B for return periods of <5 years, but larger for return periods of >5 years. This can be explained in the same way as the case of the damage potential curves in Figure 9.

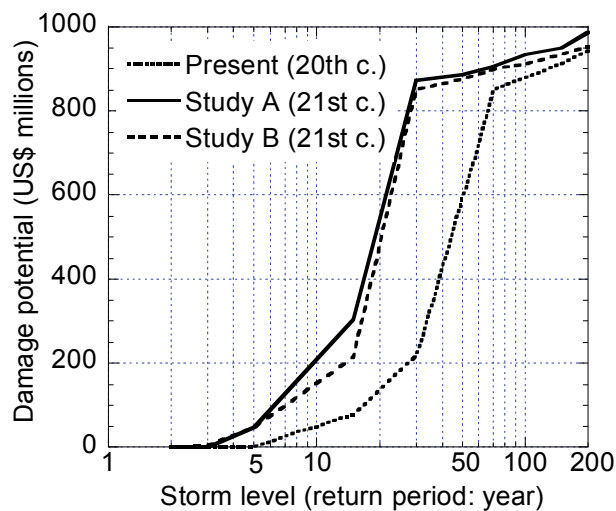


Figure 9. Damage potential curves for the 20th and 21st centuries.

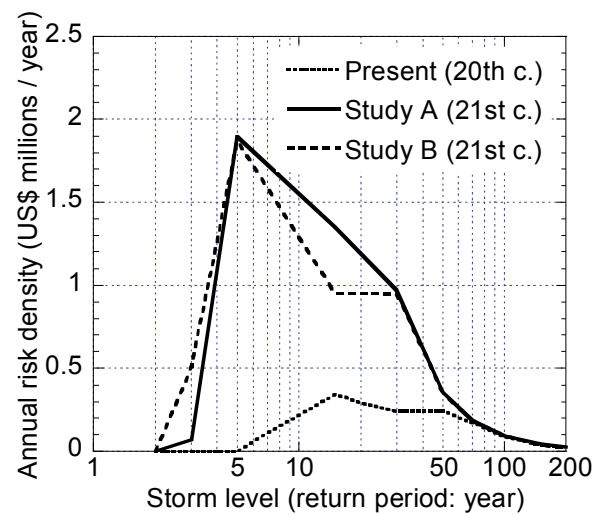


Figure 10. Annual risk density curves for the 20th and 21st centuries.

4.3 Risk cost and risk cost increase

The risk cost for global warming can be calculated by integrating the annual risk density curve shown in Figure 10 over 1- to 200-year return period. The risk cost for the 20th century, under the present design storm scenario, was computed to be approximately 24 million US\$/year. As mentioned before, this figure represents the average monetary expenditure for flood inundation damages. The risk costs of the two studies for the 21st century were calculated, integrating the two projected annual risk density curves. Figure 11 shows the calculated risk costs for the 20th and 21st centuries. The risk cost increases due to global warming were computed from the difference in risk cost between the 20th and the 21st centuries. The risk cost increase thus estimated is approximately 40 million US\$/year for Study A and 35 million US\$/year for Study B, respectively.

4.4 Risk cost increase and flood control projects

If measures that reduce the likelihood of inundation could be implemented, the inundation damage and flood risk would be reduced by these flood control projects. Table 2 shows the flood control plans with flood control reservoirs and storm infiltration facilities. Plan A0 means the present state of the catchment. Figure 2 shows the completed reservoirs R0 and the hypothetical reservoirs R1, R2, and R3. Plan A1, A2, and A3 are flood control plans using flood control reservoirs shown in Table 2. All of the hypothetical reservoirs have a storage capacity of 300 000m³. Plan D1, D2, D3, and D4 are intended to decrease the rate of impervious area introducing storm infiltration facilities. Although roof surfaces of buildings are impervious, they would be pervious if the infiltration facilities would collect all of the rainfall on them. The assumed impervious area rates are shown in Table 2.

Table 2 Flood control plans for flood risk assessment

Plan	Flood control reservoirs				Plan	Infiltration facilities (impervious area rate)				
	R0	R1	R2	R3		0.65(present)	0.60	0.55	0.50	0.45
A0	✓				D1		✓			
A1	✓	✓			D2			✓		
A2	✓	✓	✓		D3				✓	
A3	✓	✓	✓	✓	D4					✓

Morita(2009) estimated the risk cost reduction effects of hypothetical reservoirs (flood control plans:

A1, A2, and A3) and of introduction of storm infiltration facilities intended to reduce the rate of impervious area of the basin from 0.60 to 0.45 (flood control plans: D1, D2, D3, and D4). The estimated risk cost reduction for the flood control plans and corresponding capital costs are quoted from Morita (2009) in Figure 12.

The risk cost reduction and corresponding capital cost for each flood control plan are plotted along with the $B/C=1$ line. Plans using the flood control reservoirs fall below the $B/C=1$ line, whereas most of the storm infiltration plans fall above the line and more cost effective. The risk cost increase due to global climate change would be approximately 40 million US\$/year for Study A and 35 million US\$/year for Study B, respectively. Will it be possible to cope with this risk cost increase through flood control plans? The risk cost increases owing to global change are greater than the risk cost reductions of the flood control plans as shown in Figure 12. The B/C ratios of both the reservoir plans and the plans to reduce impervious area increase more moderately against capital cost and turn out to be less effective from a cost-benefit viewpoint. Thus, the assessment shows that the risk loading effect of global warming on flood control infrastructure could overbalance the risk reducing effect of currently envisioned future flood control projects.

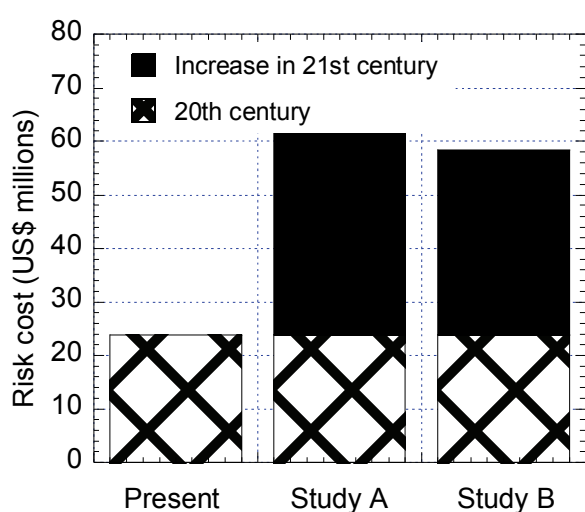


Figure 11. Annual risk cost increase due to global warming.

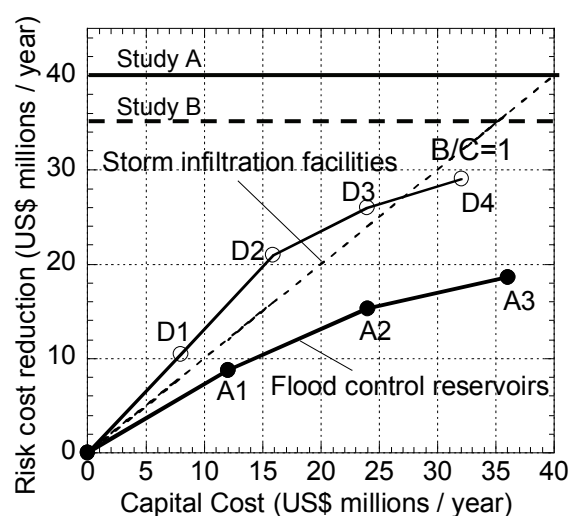


Figure 12. Risk cost reduction and capital cost for flood control projects.

5 CONCLUSIONS

The objective of this study was to present a quantification method for the assessment of flood risk increase caused by global climate change. The most important results are as follows:

- (1) A framework for a risk assessment method employing a FDPM with GIS data for quantifying the impact of climate change on the local hydrological system has been developed.
- (2) The risk assessment method was applied to estimate the risk increase effects of global warming on flood control in the Kanda River basin in Tokyo. The risk analysis quantified the flood risk, producing two curves each for the 21th and 21st centuries: the damage potential curve and the annual risk density curve.
- (3) The risk cost increase due to climate change was quantified using modified IDF curves based on probability change in precipitation under global warming conditions. The estimated risk cost could double in the 21st century. The risk loading effect of climate change on flood control infrastructure could be greater than the risk cost reduction effect of future flood control projects.

LIST OF REFERENCES

- Chow V.T., Maidment D. R., and Mays L.W. (1988). *Applied Hydrology*, MacGraw-Hill, International Edition, New York.
- Davis D. W. (2002). Risk analysis in flood damage reduction studies – The Corps Experience, *Proceedings of*

- EWRI, ASCE, Philadelphia, Pennsylvania, USA.
- DEFRA (2003). Climate adaptation: Risk, uncertainty and decision-making. *UKCIP Technical Report*, Willows, R.I. and Connell, R.K. (Eds.), UK Climate Impact Programme, UKCIP, Oxford.
- Guo J.C.Y. (2002). Overflow risk analysis for stormwater quality control basins, *Journal of Hydrological Engineering*, ASCE2002, 7(6), 428-434.
- IPCC (2007). Climate change 2007, *Forth Assessment Report Climate Change 2007 : Synthesis Report*, Topic 3, http://www.ipcc.ch/pdf/assessment-report/ar4/syr/ar4_syr.pdf [accessed 14 September 2009].
- Morita M. and Yen B.C. (2002). Modelling of conjunctive two-dimensional surface-three dimensional subsurface flows, *Journal of Hydraulic Engineering*, ASCE, **128**(2), 184-200.
- Morita M. (2008a). Risk analysis and decision-making for optimal flood protection level in urban river management, *Proceedings of the European Conference on Flood Risk Management*, "FLOODrisk 2008", CD-ROM, Oxford, UK.
- Morita M. (2008b). Flood risk analysis for determining optimal flood protection levels in urban river management. *Journal of Flood Risk Management*, **1**(3), 142-149.
- Morita M. (2009). Quantification of flood risk and its application for flood risk assessment for urban river management, *Proceedings of the 8th Urban Drainage Modeling Conference*, CD-ROM, Tokyo, Japan.
- National Institute for Land and Infrastructure Management (2004). Joint research on the variation of rainfall characteristic associated with global warming, *Technical Note of NILIM*, No.320.
- National Research Council (1989). *Improving risk communications*, National Academy Press, Washington, D.C.
- Nguyen, V-T-V., Nguyen, T-D., and Cung, A. (2007). A statistical approach to downscaling of sub-daily extreme rainfall processes for climate-related impacts studies in urban areas, *Water Science and Technology: Water Supply*, **7**(2), pp.183-192.
- Saita W. (2005). Probability change of precipitation under global warming condition, *Master degree thesis (in Japanese)*, The institute of industrial science, The university of Tokyo.
- Plate E. J. (2002). Flood risk and flood management, *Journal of Hydrology*, **267**, 2-11.
- River Bureau of the Construction Ministry (2000). *Manual for economic analysis of flood damage*.